PHYSICAL REVIEW D **88,** 055011 (2013)

One or more Higgs bosons?

Riccardo Barbieri,[1,*] Dario Buttazzo,[1,2,†] Kristjan Kannike,[1,3,‡] Filippo Sala,[1,4,§] and Andrea Tesi[1,‖]

[1]*Scuola Normale Superiore and INFN, Piazza dei Cavalieri 7, 56126 Pisa, Italy*
[2]*CERN Theory Division, CH-1211 Geneva 23, Switzerland*
[3]*National Institute of Chemical Physics and Biophysics, Rävala 10, Tallinn 10143, Estonia*
[4]*Theoretical Physics Group, Lawrence Berkeley National Laboratory, Berkeley, California 94720, USA*

(Received 30 July 2013; published 10 September 2013)

Now that one has been found, the search for signs of more scalars is a primary task of current and future experiments. In the motivated hypothesis that the extra Higgs bosons of the next-to-minimal supersymmetric Standard Model are the lightest new particles around, we outline a possible overall strategy to search for signs of the *CP*-even states. This work complements Barbieri *et al.* [Phys. Rev. D **87**, 115018 (2013)].

DOI: 10.1103/PhysRevD.88.055011 PACS numbers: 14.80.Da, 12.60.Fr, 12.60.Jv

I. INTRODUCTION

The discovery of the/a Higgs boson, $h_{\rm LHC}$, with a mass of about 126 GeV and Standard-Model-like properties [1–5] raises a clear question: is it the coronation of the Standard Model (SM) or a first step into yet largely unexplored territory? The answer to this question—whose relation with the absence so far of any signal of new physics does not need to be illustrated—is in some sense paradoxical. While the newly found resonance completes the SM spectrum, thus representing a major milestone in the entire history of particle physics, there are still good reasons to think that its discovery may not be the end of the story. The many well-known problems that the finding of the resonance—viewed as the Higgs boson of the SM—leaves unresolved are one type of these reasons. Quite independently and in fact on more general grounds, now that a scalar particle has been found one may wonder if and why it should be alone and not part of an extended Higgs system. Since we know of no strong argument in favor of a single scalar particle, it is justified to think that the search for signs of extra scalars is a primary task of current and future experiments.

A motivated example of an extended Higgs system is the next-to-minimal supersymmetric Standard Model (NMSSM), which adds to a usual Higgs doublet one further doublet and one complex singlet under the $\mathrm{SU}(2) \times \mathrm{U}(1)$ gauge group—all parts of corresponding chiral supermultiplets—so as to allow a supersymmetric gauge-invariant Yukawa-like coupling $\lambda S H_u H_d$ [6] (see Ref. [7] for a review and references). In spite of the presence of (broken) supersymmetry, the Higgs sector of the NMSSM is not free from the problem common to the introduction of a scalar sector in any gauge theory: the significant number of free parameters that describe their masses and interactions, of which the Yukawa couplings in the SM are a prototype example. In turn this explains the difficulty of finding a simple enough description of the related phenomenology, as well as the extended literature on the subject.[1] The purpose of this work is to outline a possible overall strategy to search for signs of the *CP*-even extra states of the NMSSM Higgs sector. This paper must be viewed as a complement of Ref. [25], to which we add i) the consideration of the case in which one state exists below $h_{\rm LHC}$, ii) the expected sensitivity on the overall parameter space of the measurements of the signal strengths of $h_{\rm LHC}$ at LHC14 with their projected errors, and iii) the consideration of the impact of the electroweak precision tests (EWPT) on the different situations. To keep things comprehensive we will have to make some simplifying assumptions, which we shall be careful to specify whenever needed.

II. REFERENCE EQUATIONS

For the ease of the reader we summarize in this section the definitions and the reference equations that we shall use to describe the relation between the physical observables and the parameters of a generic NMSSM.

Assuming a negligibly small *CP* violation in the Higgs sector, the original scalar fields $\mathcal{H} = (H_d^0, H_u^0, S)^T$ are related to the three *CP*-even physical mass eigenstates $\mathcal{H}_{\rm ph} = (h_3, h_1, h_2)^T$ by

$$\mathcal{H} = R_\alpha^{12} R_\gamma^{23} R_\sigma^{13} \mathcal{H}_{\rm ph} \equiv R \mathcal{H}_{\rm ph}, \tag{2.1}$$

where R_θ^{ij} is the rotation matrix in the ij sector by the angle $\theta = \alpha, \gamma, \sigma$. We shall denote the resonance found at LHC by h_1.

*barbieri@sns.it
†dario.buttazzo@sns.it
‡kannike@cern.ch
§filippo.sala@sns.it
‖andrea.tesi@sns.it

[1]For a partial list of recent references, see Refs. [8–24].

In full generality the mixing angles $\delta \equiv \alpha - \beta + \pi/2$, γ, σ can be expressed in terms of the masses m_{h_1,h_2,h_3} and $m_{H^\pm}$, the charged Higgs boson mass, as [25][2]

$$s_\gamma^2 = \frac{\det M^2 + m_{h_1}^2(m_{h_1}^2 - \mathrm{tr}M^2)}{(m_{h_1}^2 - m_{h_2}^2)(m_{h_1}^2 - m_{h_3}^2)}, \tag{2.2}$$

$$s_\sigma^2 = \frac{m_{h_2}^2 - m_{h_1}^2}{m_{h_2}^2 - m_{h_3}^2} \frac{\det M^2 + m_{h_3}^2(m_{h_3}^2 - \mathrm{tr}M^2)}{\det M^2 - m_{h_2}^2 m_{h_3}^2 + m_{h_1}^2(m_{h_2}^2 + m_{h_3}^2 - \mathrm{tr}M^2)}, \tag{2.3}$$

$$\begin{aligned} s_{2\delta} = & [2s_\sigma c_\sigma s_\gamma (m_{h_3}^2 - m_{h_2}^2)(2\tilde{M}_{11}^2 - m_{h_1}^2 c_\gamma^2 - m_{h_2}^2(s_\gamma^2 + s_\sigma^2 c_\gamma^2) \\ & - m_{h_3}^2(c_\sigma^2 + s_\gamma^2 s_\sigma^2)) + 2\tilde{M}_{12}^2(m_{h_3}^2(c_\sigma^2 - s_\gamma^2 s_\sigma^2) \\ & + m_{h_2}^2(s_\sigma^2 - s_\gamma^2 c_\sigma^2) - m_{h_1}^2 c_\gamma^2)][(m_{h_3}^2 - m_{h_2}^2 s_\gamma^2 - m_{h_1}^2 c_\gamma^2)^2 \\ & + (m_{h_2}^2 - m_{h_3}^2)^2 c_\gamma^4 s_\sigma^4 + 2(m_{h_2}^2 - m_{h_3}^2) \\ & \times (m_{h_3}^2 + m_{h_2}^2 s_\gamma^2 - m_{h_1}^2(1 + s_\gamma^2))c_\gamma^2 s_\sigma^2]^{-1}, \end{aligned} \tag{2.4}$$

where $s_\theta = \sin\theta$, $c_\theta = \cos\theta$, M^2 is the 2×2 submatrix in the 12 sector of the full 3×3 squared-mass matrix $\mathcal{M}^2$ of the neutral CP-even scalars in the $\mathcal{H}$ basis,

$$M^2 = \begin{pmatrix} m_Z^2 c_\beta^2 + m_A^2 s_\beta^2 & (2v^2\lambda^2 - m_A^2 - m_Z^2)c_\beta s_\beta \\ (2v^2\lambda^2 - m_A^2 - m_Z^2)c_\beta s_\beta & m_A^2 c_\beta^2 + m_Z^2 s_\beta^2 + \delta_t^2 \end{pmatrix}, \tag{2.5}$$

and $\tilde{M}^2 = R_{\beta-\pi/2} M^2 R^t_{\beta-\pi/2}$ in Eq. (2.4). In Eq. (2.5)

$$m_A^2 = m_{H^\pm}^2 - m_W^2 + \lambda^2 v^2, \tag{2.6}$$

where $v \simeq 174$ GeV, and

$$\delta_t^2 \equiv \Delta_t^2 / s_\beta^2 \tag{2.7}$$

is the well-known effect of the top-stop loop corrections to the quartic coupling of H_u. We neglect the analogous correction to Eq. (2.6), which lowers $m_{H^\pm}$ by less than 3 GeV for stop masses below 1 TeV. More importantly we have also not included in Eq. (2.5) the one-loop corrections to the 12 and 11 entries, respectively proportional to the first and second power of $(\mu A_t)/\langle m_{\tilde{t}}^2 \rangle$, to which we shall return.

We shall in particular be interested in two limiting cases:

(i) H decoupled: $m_{h_3} \gg m_{h_1,h_2}$ and σ, $\delta \equiv \alpha - \beta + \pi/2 \to 0$,

(ii) Singlet decoupled: $m_{h_2} \gg m_{h_1,h_3}$ and σ, $\gamma \to 0$.

However, we use Eqs. (2.2), (2.3), and (2.4) to control the size of the deviations from the limiting cases when the heavier mass is lowered. In the two respective cases the reference equations are the following:

(i) H decoupled:

$$s_\gamma^2 = \frac{m_{hh}^2 - m_{h_1}^2}{m_{h_2}^2 - m_{h_1}^2}, \tag{2.8}$$

where

$$m_{hh}^2 = m_Z^2 c_{2\beta}^2 + \lambda^2 v^2 s_{2\beta}^2 + \Delta_t^2; \tag{2.9}$$

(ii) Singlet decoupled:

$$s_{2\alpha} = s_{2\beta} \frac{2\lambda^2 v^2 - m_Z^2 - m_A^2|_{m_{h_1}}}{m_A^2|_{m_{h_1}} + m_Z^2 + \delta_t^2 - 2m_{h_1}^2}, \tag{2.10}$$

$$m_{h_3}^2 = m_A^2|_{m_{h_1}} + m_Z^2 + \delta_t^2 - m_{h_1}^2, \tag{2.11}$$

where

$$m_A^2|_{m_{h_1}} = \frac{\lambda^2 v^2(\lambda^2 v^2 - m_Z^2)s_{2\beta}^2 - m_{h_1}^2(m_{h_1}^2 - m_Z^2 - \delta_t^2) - m_Z^2 \delta_t^2 c_\beta^2}{m_{hh}^2 - m_{h_1}^2}. \tag{2.12}$$

All the equations in this section are valid in a generic NMSSM. Specific versions of it may limit the range of the physical parameters $m_{h_{1,2,3}}$, $m_{H^\pm}$, and α, γ, σ, but it cannot affect any of these equations.

III. SINGLET DECOUPLED

From Eqs. (2.10), (2.12), and (2.6), since m_{h_1} is known, m_{h_3}, m_{H^+} and the angle δ are functions of $(\tan\beta, \lambda, \Delta_t)$. From our point of view the main motivation for considering the NMSSM is in the possibility to account for the mass of h_{LHC} with not too big values of the stop masses. For this reason we take $\Delta_t = 75$ GeV, which can be obtained, e.g., for an average stop mass of about 700 GeV. In turn—as will be seen momentarily—the

[2]Notice that Eq. (2.4) is completely equivalent to the expression for $\sin 2\alpha$ in Eq. (2.10) of Ref. [25].

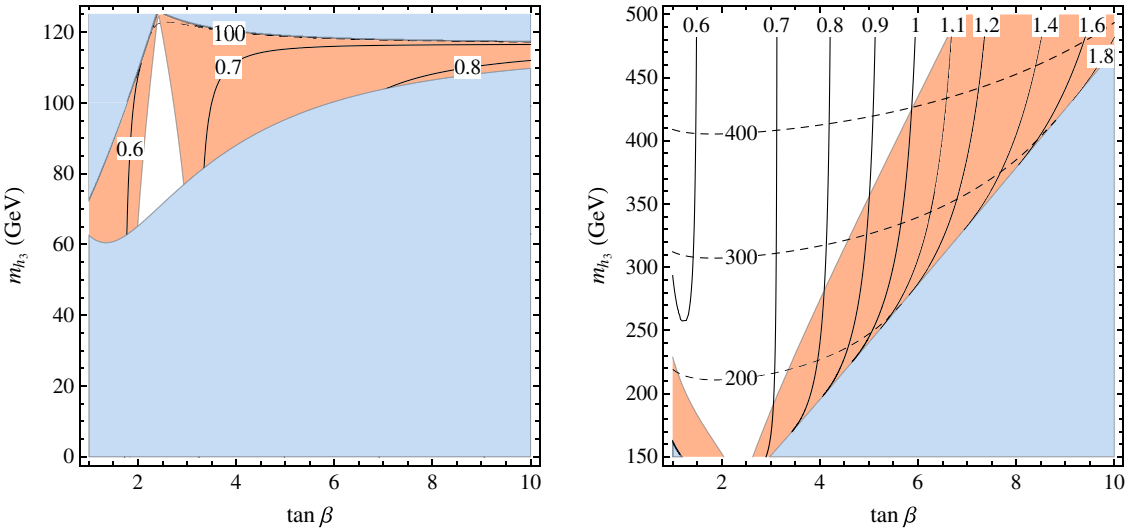

FIG. 1 (color online). Singlet decoupled. Isolines of λ (solid) and $m_{H^\pm}$ (dashed). Left: $h_{\rm LHC} > h_3$. Right: $h_{\rm LHC} < h_3$. The orange (medium gray) region is excluded at 95% C.L. by the experimental data for the signal strengths of $h_1 = h_{\rm LHC}$. The blue (light gray) region is unphysical.

consistency of Eqs. (2.10), (2.11), and (2.12) requires not too small values of the coupling λ. In fact, it turns out that for any value of $\Delta_t \lesssim 85$ GeV, the dependence on Δ_t itself can be neglected, so that m_{h_3}, $m_{H^\pm}$, and δ are determined by $\tan\beta$ and λ only. For the same reason it is legitimate to neglect the one-loop corrections to the 11 and 12 entries of the mass matrix, Eq. (2.5), as long as $(\mu A_t)/\langle m_t^2\rangle \lesssim 1$, which is again motivated by naturalness.

From all this we can represent in Fig. 1 the allowed regions in the plane ($\tan\beta$, m_{h_3}) and the isolines of λ and $m_{H^\pm}$ for both $h_3 < h_{\rm LHC} (< h_3 (= S))$ and for $h_{\rm LHC} < h_3 (< h_3 (= S))$, which were already considered in Ref. [25]. At the same time the knowledge of δ at every point of the same ($\tan\beta$, m_{h_3}) plane fixes the couplings of h_3 and $h_{\rm LHC}$, which allows one to draw the currently excluded regions from the measurements of the signal strengths of $h_{\rm LHC}$. We do not include any supersymmetric loop effects other than the ones that give rise to Eq. (2.5). As in Ref. [25], to make the fit of all the data collected so far from ATLAS, CMS, and Tevatron, we adapt the code provided by the authors of Ref. [26]. Negative searches at LHC of $h_3 \to \bar\tau\tau$ may also exclude a further portion of the parameter space for $h_3 > h_{\rm LHC}$. Note that, as anticipated, in every case λ is bound to be above about 0.6. To go to lower values of λ would require considering $\Delta_t \gtrsim 85$ GeV, i.e., heavier stop. On the other hand, in this singlet-decoupled case lowering λ and raising Δ_t makes the NMSSM close to the minimal supersymmetric Standard Model (MSSM), to which we shall return.

When drawing the currently excluded regions in Fig. 1, we are not considering the possible decays of $h_{\rm LHC}$ and/or of h_3 into invisible particles—such as dark matter—or into any undetected final state because of background, like, e.g., a pair of light pseudoscalars. The existence of such decays, however, would not alter in any significant way the excluded regions from the measurements of the signal strengths of $h_{\rm LHC}$, which would all be modified by a common factor $(1 + \Gamma_{\rm inv}/\Gamma_{\rm vis})^{-1}$. This is because the inclusion in the fit of the LHC data of an invisible branching ratio of $h_{\rm LHC}$, $\mathrm{BR}_{\rm inv}$, leaves essentially unchanged the allowed range for δ at different $\tan\beta$ values, provided $\mathrm{BR}_{\rm inv} \lesssim 0.2$.

The significant constraint set on Fig. 1 by the current measurements of the signal strengths of $h_{\rm LHC}$ suggests that an improvement of such measurements, as foreseen in the coming stage of LHC, could lead to an effective exploration of most of the relevant parameter space. To quantify this we have considered the impact on the fit of the measurements of the signal strengths of $h_{\rm LHC}$ with the projected errors at LHC14 with 300 fb^{-1} by ATLAS [27] and CMS [28], shown in Table I. The result is shown in Fig. 2, again for both $h_3 < h_{\rm LHC} (< h_2 (= S))$ and for $h_{\rm LHC} < h_3 (< h_2 (= S))$, assuming SM central values for the signal strengths.

Needless to say, the direct search of the extra CP-even states will be essential either in the presence of possible indirect evidence from the signal strengths or to fully cover the parameter space for $h_3 > h_{\rm LHC}$. To this end, under the

TABLE I. Projected uncertainties of the measurements of the signal strengths of $h_{\rm LHC}$, normalized to the SM, at the 14 TeV LHC with 300 fb^{-1}.

	ATLAS	CMS
$h \to \gamma\gamma$	0.16	0.15
$h \to ZZ$	0.15	0.11
$h \to WW$	0.30	0.14
$Vh \to Vb\bar b$	–	0.17
$h \to \tau\tau$	0.24	0.11
$h \to \mu\mu$	0.52	–

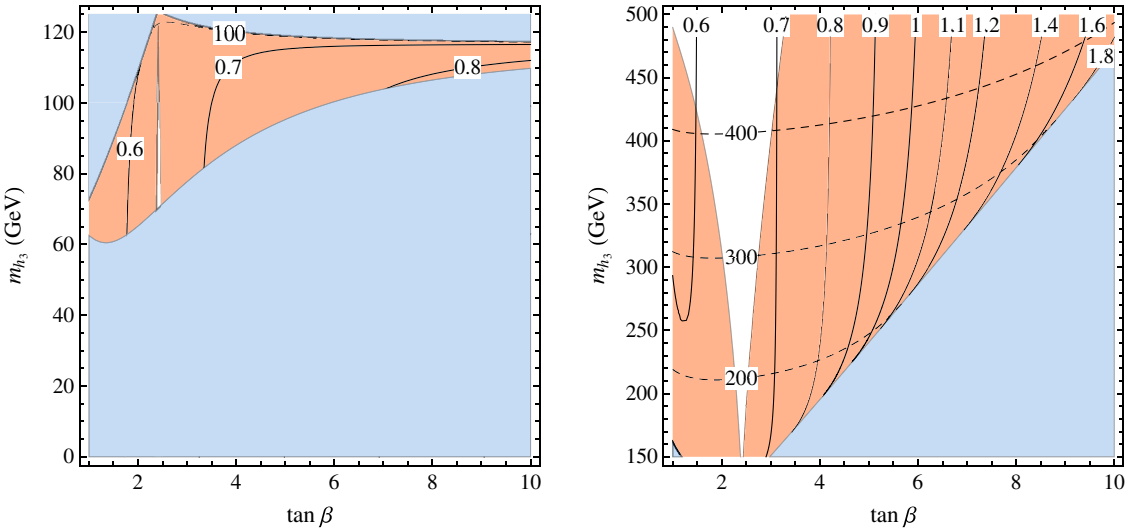

FIG. 2 (color online). Singlet decoupled. Isolines of λ (solid) and $m_{H^\pm}$ (dashed). Left: $h_{\rm LHC} > h_3$. Right: $h_{\rm LHC} < h_3$. The orange (medium gray) region would be excluded at 95% C.L. by the experimental data for the signal strengths of $h_1 = h_{\rm LHC}$ with SM central values and projected errors at the LHC14 as discussed in the text. The blue (light gray) region is unphysical.

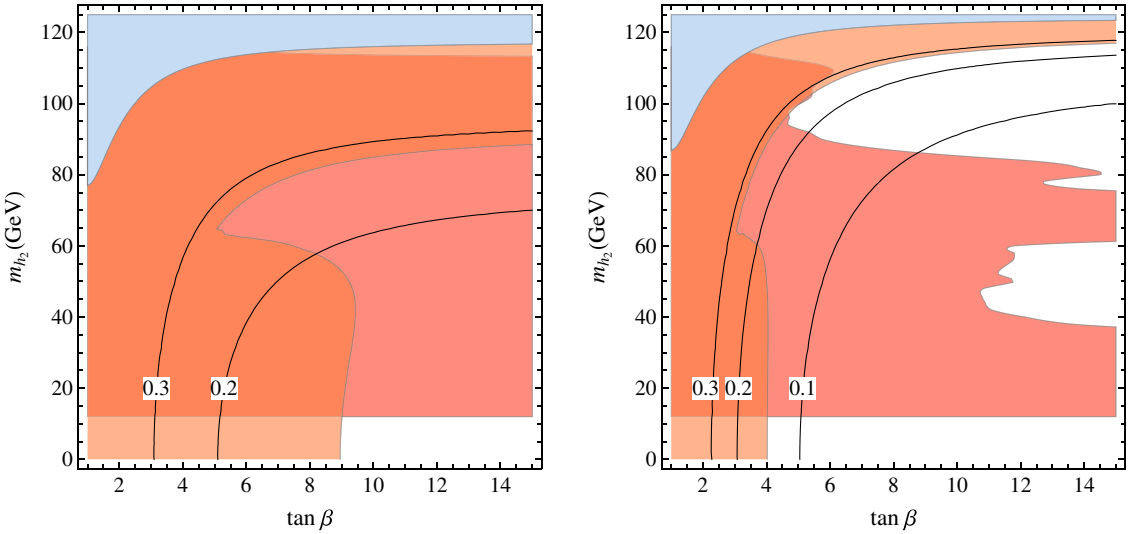

FIG. 3 (color online). H decoupled. Isolines of s^2_γ. $\lambda = 0.1$ and $v_S = v$. Left: $\Delta_t = 75$ GeV. Right: $\Delta_t = 85$ GeV. The orange (medium gray) and blue (light gray) regions are as in Fig. 1. The red (darker gray) region is excluded by LEP direct searches for $h_2 \to b\bar{b}$.

stated assumptions, all production cross sections and branching ratios for the h_3 state are determined at every point of the $(\tan\beta, m_{h_3})$ plane.

IV. H DECOUPLED

As we are going to see, the situation changes significantly when considering the H-decoupled case where the singlet S mixes with the doublet with SM couplings. By comparing Eq. (2.8) with Eq. (2.10), we note first that in this case there is only a single relation between the mixing angle γ and the mass of the extra CP-even state m_{h_2}, involving $\tan\beta$, λ, and Δ_t. Since the case of $h_{\rm LHC} < h_2 (< h_3 (= H))$ has been extensively discussed in Ref. [25], here we concentrate on the case of $h_2 < h_{\rm LHC} (< h_3 (= H))$ and we consider both the low- and the large-λ case.

The low-λ case ($\lambda = 0.1$) is shown in Fig. 3 for two values of Δ_t together with the isolines of s^2_γ. Due to the singlet nature of S it is straightforward to see that the couplings of $h_1 = h_{\rm LHC}$ and h_2 to fermions or to vector-boson pairs, $VV = WW, ZZ$, normalized to the same couplings of the SM Higgs boson, are given by

$$\frac{g_{h_1 ff}}{g^{\rm SM}_{hff}} = \frac{g_{h_1 VV}}{g^{\rm SM}_{hVV}} = c_\gamma, \qquad \frac{g_{h_2 ff}}{g^{\rm SM}_{hff}} = \frac{g_{h_2 VV}}{g^{\rm SM}_{hVV}} = -s_\gamma. \tag{4.1}$$

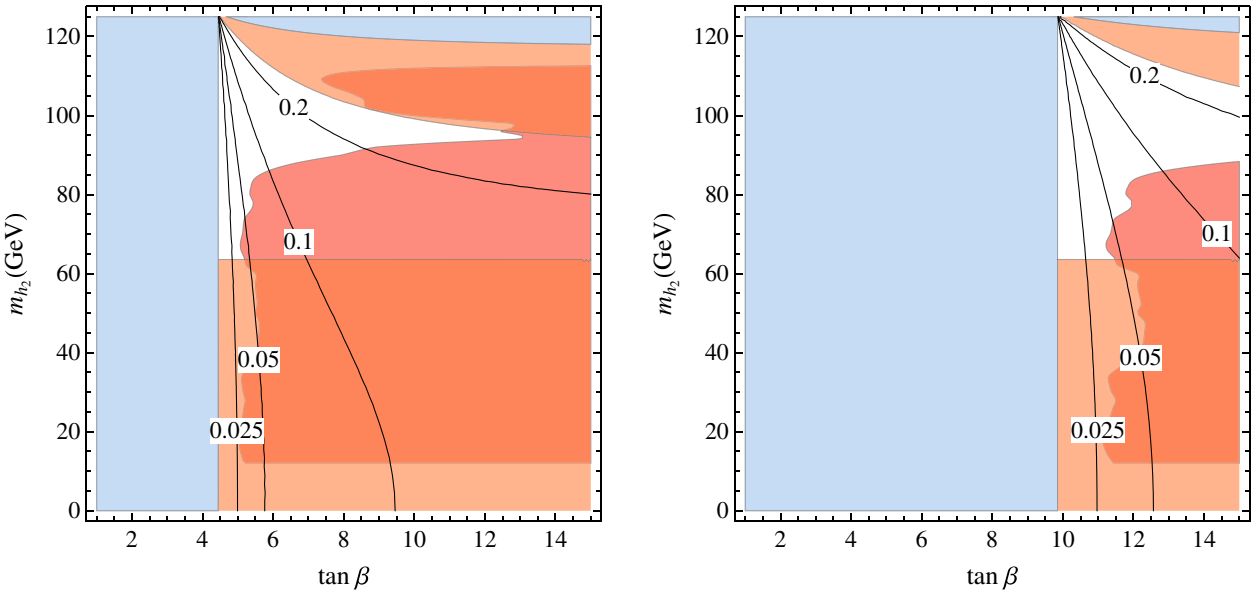

FIG. 4 (color online). H decoupled. Isolines of s_γ^2. $\Delta_t = 75$ GeV and $v_S = v$. Left: $\lambda = 0.8$. Right: $\lambda = 1.4$. The orange (medium gray) and blue (light gray) regions are as in Fig. 1. The red (darker gray) region is excluded by LEP direct searches for $h_2 \to b\bar{b}$.

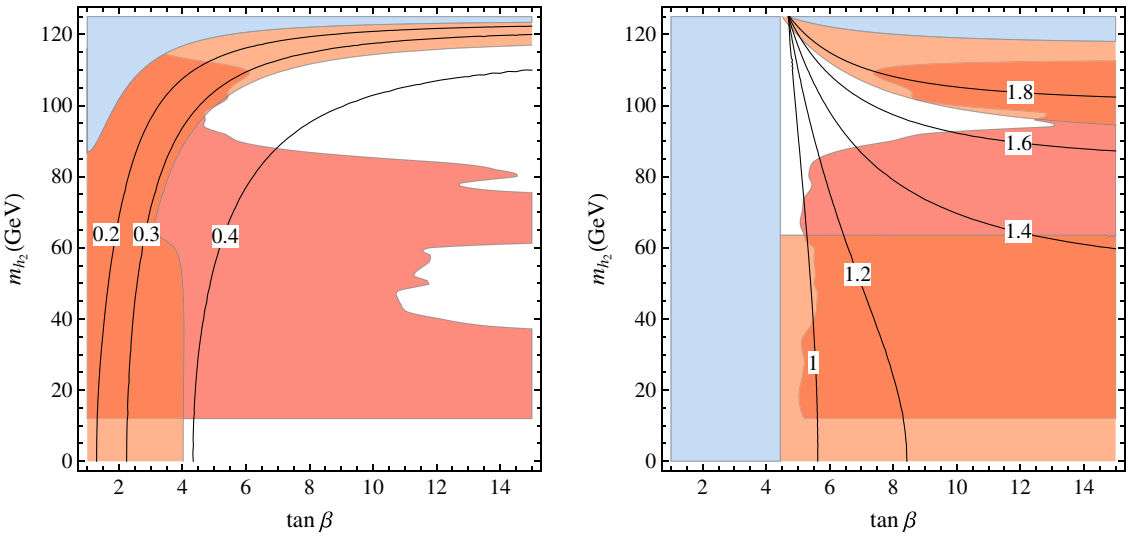

FIG. 5 (color online). H decoupled. Isolines of $g_{h^3}/g_{h^3}|_{\rm SM}$. Left: $\lambda = 0.1$, $\Delta_t = 85$ GeV and $v_S = v$. Right: $\lambda = 0.8$, $\Delta_t = 75$ GeV and $v_S = v$. The orange (medium gray) and blue (light gray) regions are as in Fig. 1. The red (darker gray) region is excluded by LEP direct searches for $h_2 \to b\bar{b}$.

As a consequence for $m_{h_2} > m_{h_{\rm LHC}}/2$ none of the branching ratios of $h_1 = h_{\rm LHC}$ and h_2 get modified with respect to the ones of the SM Higgs boson with the corresponding mass, whereas their production cross sections are reduced by a common factor c_γ^2 or s_γ^2, respectively, for $h_1 = h_{\rm LHC}$ and h_2. The current fit of the signal strengths measured at LHC constrain $s_\gamma^2 < 0.22$ at 95% C.L., which explains the lighter excluded regions in Fig. 3. The red regions are due to the negative searches of $h_2 \to \bar{b}b$ at LEP [29]. As in the previous case we do not include any invisible decay mode except for $h_{\rm LHC} \to h_2 h_2$ when kinematically allowed.[3] Here an invisible branching ratio of $h_{\rm LHC}$, $\mathrm{BR}_{\rm inv}$, would strengthen the bound on the mixing angle to $s_\gamma^2 < (0.22 - 0.78\mathrm{BR}_{\rm inv})$.

[3]To include $h_{\rm LHC} \to h_2 h_2$ we rely on the triple Higgs couplings as computed by retaining only the λ^2 contributions. This is a defendable approximation for λ close to unity, where $h_{\rm LHC} \to h_2 h_2$ is important. In the low-λ case the λ^2 approximation can only be taken as indicative, but there $h_{\rm LHC} \to h_2 h_2$ is less important.

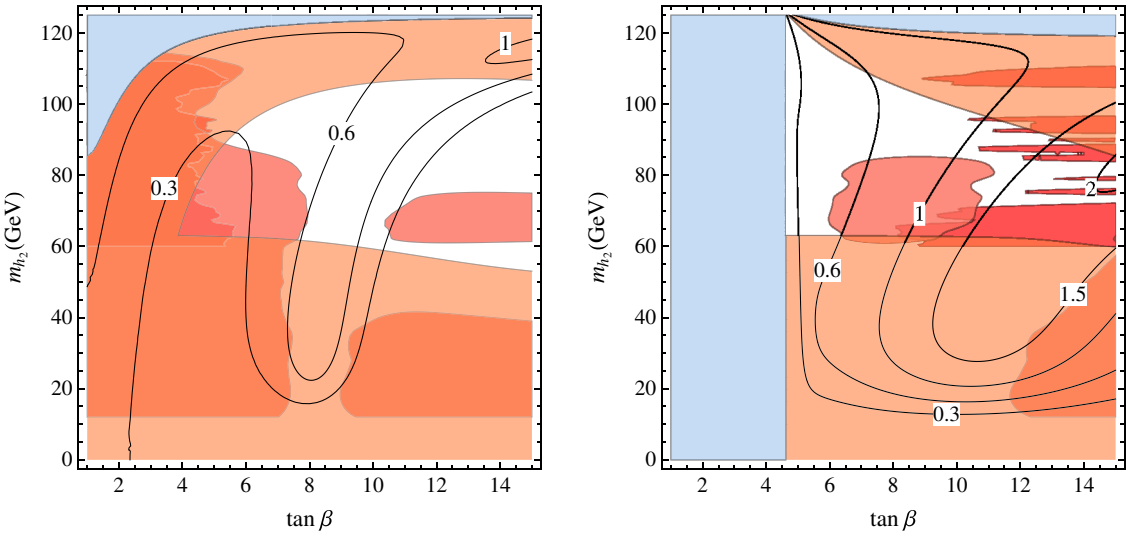

FIG. 6 (color online). Fully mixed situation. Isolines of the signal strength of $h_2 \to \gamma\gamma$ normalized to the SM. We take $m_{h_3} = 500$ GeV, $s_\sigma^2 = 0.001$, and $v_s = v$. Left: $\lambda = 0.1$, $\Delta_t = 85$ GeV. Right: $\lambda = 0.8$, $\Delta_t = 75$ GeV. The orange (medium gray) and blue (light gray) regions are as in Fig. 1. The red (darker gray) and dark red regions are excluded by LEP direct searches for $h_2 \to b\bar{b}$ and $h_2 \to$ hadrons, respectively.

For λ close to unity we take as in the singlet-decoupled case $\Delta_t = 75$ GeV, but any choice lower than this would not change the conclusions. The currently allowed region is shown in Fig. 4 for two values of λ. Note that, for large λ, no solution is possible at low enough $\tan\beta$, since, before mixing, m_{hh}^2 in Eq. (2.9) has to be below the mass squared of $h_{\rm LHC}$.

How will it be possible to explore the regions of parameter space currently still allowed in this $h_2 < h_{\rm LHC} (< h_3 (= H))$ case in view of the reduced couplings of the lighter state? Unlike in the singlet-decoupled case, the improvement in the measurements of the signal strengths of $h_{\rm LHC}$ is not going to play a major role. Based on the projected sensitivity of Table I, the bound on the mixing angle will be reduced to $s_\gamma^2 < 0.15$ at 95% C.L. A significant deviation from the case of the SM can occur in the cubic $h_{\rm LHC}$ coupling, $g_{h_1^3}$, as shown in Fig. 5. The LHC14 in the high-luminosity regime is expected to get enough sensitivity to be able to see such deviations [27,30,31]. At that point, on the other hand, the searches for directly produced s-partners should have already given some clear indications of the relevance of the entire picture.

For completeness we recall from Ref. [25] that the parameter space in the case $h_{\rm LHC} < h_2 (< h_3 (= H))$ is still largely unexplored at $\lambda = 0.7$-1. Most promising in this case are the direct searches of h_2 with gluon-fusion production cross sections at LHC14 in the picobarn range and a large branching ratio—when allowed by phase space—into a pair of $h_{\rm LHC}$'s. Furthermore, here as well large deviations from the SM value can occur in the cubic $h_{\rm LHC}$ coupling.

V. FULLY MIXED CASE AND THE $\gamma\gamma$ SIGNAL

The phenomenological exploration of the situation considered in the previous section could be significantly influenced if the third state, i.e., the doublet H, were not fully decoupled. As an example we still consider the case of a state h_2 lighter than $h_{\rm LHC}$, lowering m_{h_3} to 500 GeV, to see if it could have an enhanced signal strength into $\gamma\gamma$. Using Eqs. (2.2), (2.3), and (2.4), for fixed values of σ, λ, and Δ_t, the two remaining angles α (or $\delta = \alpha - \beta + \pi/2$) and γ are determined at any point of the $(\tan\beta, m_{h_2})$ plane and so are all the branching ratios of h_2 and of $h_{\rm LHC}$. More precisely δ is fixed up to the sign of $s_\sigma c_\sigma s_\gamma$ [see the first line of Eq. (2.4)], which is the only physical sign that enters the observables we are considering.

The corresponding situation is represented in Fig. 6, for two choices of λ and Δ_t (the choice $\lambda = 0.1$ was recently discussed in Ref. [22]). The sign of $s_\sigma c_\sigma s_\gamma$ has been taken negative in order to suppress $\mathrm{BR}(h_2 \to b\bar{b})$. This constrains s_σ^2 to be very small in order to leave a region still not excluded by the signal strengths of $h_{\rm LHC}$, with δ small and negative. To get a signal strength for $h_2 \to \gamma\gamma$ close to the SM one for the corresponding mass is possible for a small enough value of s_γ^2, while the dependence on m_{h_3} is weak for values of m_{h_3} greater than 500 GeV. Note that the suppression of the coupling of h_2 to b quarks makes it necessary to consider the negative LEP searches for $h_2 \to$ hadrons [32], which have been performed down to $m_{h_2} = 60$ GeV.

Looking at the similar problem when $h_2 > h_{\rm LHC}$, we find it harder to get a signal strength close to the SM one, although this might be possible for a rather special choice of the parameters.[4] Our purpose here is more to show that in the fully mixed situation the role of the measured signal

[4]An increasing significance of the excess found by CMS [33] at 136 GeV would motivate such a special choice.

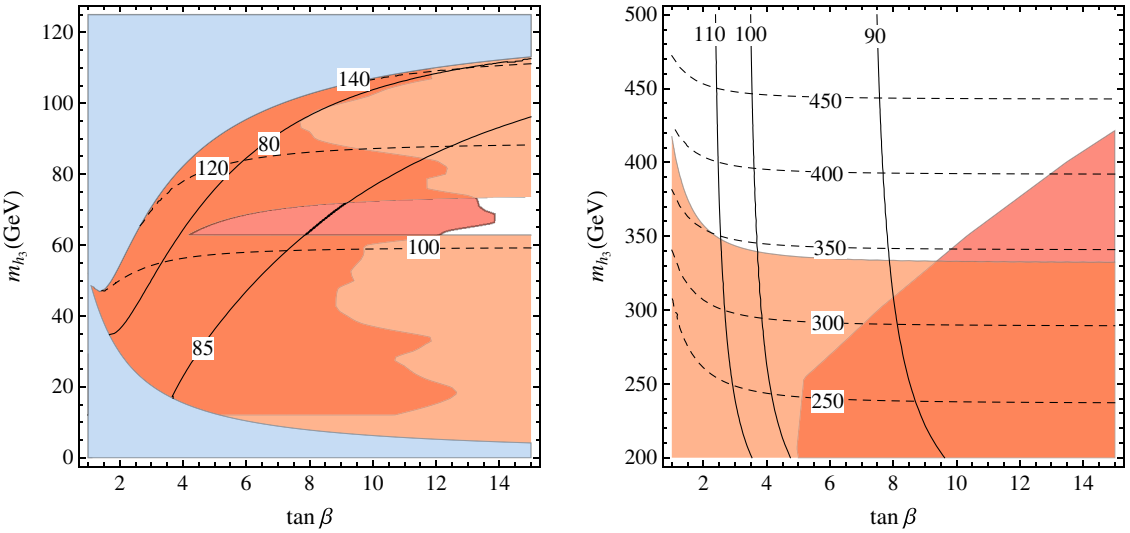

FIG. 7 (color online). MSSM. Isolines of Δ_t (solid) and $m_{H^\pm}$ (dashed) at $(\mu A_t)/\langle m_{\tilde{t}}^2 \rangle \ll 1$. Left: $h_{\rm LHC} > h_3$; the red (darker gray) region is excluded by LEP direct searches for $h_3 \to b\bar{b}$. Right: $h_{\rm LHC} < h_3$; the red (darker gray) region is excluded by CMS direct searches for $A, H \to \tau^+\tau^-$ [35]. The orange (medium gray) and blue (light gray) regions are as in Fig. 1.

strengths of $h_{\rm LHC}$—either current or foreseen—plays a crucial role.

VI. ELECTROWEAK PRECISION TESTS

One may ask if the EWPT set some further constraint on the parameter space explored so far. We have directly checked that this is not the case in any of the different situations illustrated in the various figures. The reason is different in the singlet-decoupled and in the H-decoupled cases.

In the H-decoupled case the reduced couplings of $h_{\rm LHC}$ to the weak bosons lead to well-known asymptotic formulas for the corrections to the $\hat{S}$ and $\hat{T}$ parameters [34],

$$\Delta\hat{S} = +\frac{\alpha}{48\pi s_w^2} s_\gamma^2 \log\frac{m_{h_2}^2}{m_{h_{\rm LHC}}^2},$$
$$\Delta\hat{T} = -\frac{3\alpha}{16\pi c_w^2} s_\gamma^2 \log\frac{m_{h_2}^2}{m_{h_{\rm LHC}}^2}, \tag{6.1}$$

which are valid when m_{h_2} is sufficiently heavier than $h_{\rm LHC}$. The correlation of s_γ^2 with m_{h_2} given in Eq. (2.8) leads therefore to a rapid decoupling of these effects. The one-loop effect on $\hat{S}$ and $\hat{T}$ also becomes vanishingly small as m_{h_2} and $h_{\rm LHC}$ get close to each other, since in the degenerate limit any mixing can be redefined away and only the standard doublet contributes as in the SM.

In the singlet-decoupled case the mixing between the two doublets can in principle lead to more important effects, which are however limited by the constraint on the mixing angle α or the closeness to zero of $\delta = \alpha - \beta + \pi/2$ already demanded by the measurements of the signal strengths of $h_{\rm LHC}$.[5] Since in the $\delta = 0$ limit every extra effect on $\hat{S}$ and $\hat{T}$ vanishes, this explains why the EWPT do not impose further constraints on the parameter space that we have considered.

VII. THE MSSM FOR COMPARISON

As recalled in Sec. III, it is interesting to consider the MSSM, i.e., the $\lambda = 0$ limit of the NMSSM in the singlet-decoupled case, using the same language as much as possible. The analogue of Fig. 1 is shown in Fig. 7. From the point of view of the parameter space the main difference is that instead of λ we use Δ_t as an effective parameter. As expected, both the left and right panels of Fig. 7 make clear that a large value of Δ_t is needed to make the MSSM consistent with a 125 GeV Higgs boson.

At the same time, and even more than in the NMSSM case, the projection of the measurements of the signal strengths of $h_{\rm LHC}$ is expected to scrutinize most of the parameter space. We have checked that this is indeed the case with the indirect sensitivity to m_{h_3} in the right panel of Fig. 7, which will be excluded up to about 1 TeV, as well as with the closure of the white region on the left side of the same figure. Notice that a similar exclusion will also hold for the CP-odd and charged Higgs bosons, whose masses are fixed in terms of that of h_3. A warning should be kept in mind, however, relevant to the case $h_3 < h_{\rm LHC}$: the

[5]Notice that in the fully mixed situation there may be relevant regions of the parameter space still allowed by the fit with a largish δ (see, e.g., Fig. 1 of Ref. [25]). This could further constrain the small allowed regions, but the precise contributions to the EWPT depend on the value of the masses of the CP-odd scalars, which in the generic NMSSM are controlled by further parameters.

one-loop corrections to the mass matrix controlled by $(\mu A_t)/\langle m_{\tilde{t}}^2\rangle$ modify the left side of Fig. 7 for $(\mu A_t)/\langle m_{\tilde{t}}^2\rangle \gtrsim 1$, changing in particular the currently and projected allowed regions.

VIII. SUMMARY AND CONCLUSIONS

Given the current experimental information, the Higgs sector of the NMSSM appears to allow a minimally fine-tuned description of electroweak symmetry breaking, at least in the context of supersymmetric extensions of the SM. Motivated by this fact and complementing Ref. [25], we have outlined a possible overall strategy to search for signs of the *CP*-even states by suggesting a relatively simple analytic description of four different situations:

(i) Singlet decoupled, $h_3 < h_{\rm LHC} < h_2 (= S)$;
(ii) Singlet decoupled, $h_{\rm LHC} < h_3 < h_2 (= S)$;
(iii) H decoupled, $h_2 < h_{\rm LHC} < h_3 (= H)$;
(iv) H decoupled, $h_{\rm LHC} < h_2 < h_3 (= H)$.

To make this possible at all we have made some simplifying assumptions on the parameter space, which are motivated by naturalness requirements and have been in any case specified whenever needed. In our view the advantages of having an overall coherent analytic picture justify the introduction of these assumptions.

Not surprisingly, a clear difference emerges between the singlet-decoupled and the H-decoupled cases: the influence on the signal strengths of $h_{\rm LHC}$ of the mixing with a doublet or with a singlet makes the relative effects visible at different levels. A quantitative estimate of the sensitivity of the foreseen measurements at LHC14 with 300 fb^{-1} makes it likely that the singlet-decoupled case will be thoroughly explored, while the singlet-mixing effects could remain hidden. We also found that, in the MSSM with $(\mu A_t)/\langle m_{\tilde{t}}^2\rangle \lesssim 1$, the absence of deviations in the $h_{\rm LHC}$ signal strengths would push the mass of the other Higgs bosons up to a TeV. Needless to say, in any case the direct searches will be essential with a variety of possibilities discussed in the literature. As an example we have underlined the significance of $h_2 \to h_{\rm LHC} h_{\rm LHC}$ in the $h_{\rm LHC} < h_2 < h_3 (= H)$ case. It is also interesting that, in the H-decoupled case, large deviations from the SM value are possible in the triple Higgs coupling $g^3_{h_{\rm LHC}}$, contrary to the S-decoupled and MSSM cases. More in general it is useful to observe that the framework outlined in this work makes it possible to describe the impact of the various direct searches in a systematic way, together with the indirect ones in the $h_{\rm LHC}$ couplings. Finally, in the case of a positive signal, direct or indirect, it may be important to try to interpret it in a fully mixed scheme, involving all three *CP*-even states. To this end the analytic relations of the mixing angles to the physical masses given in Eqs. (2.2), (2.3), and (2.4) offer a useful tool, as illustrated in the examples of a $\gamma\gamma$ signal in Fig. 6.

It will be interesting to follow the progression of the searches of the Higgs system of the NMSSM, directly or indirectly through the more precise measurements of the properties of the state already found at the LHC.

ACKNOWLEDGMENTS

We would like to thank Pietro Slavich for useful discussions. This work is supported in part by the European Programme "Unification in the LHC Era", Contract No. PITN-GA-2009-237920 (UNILHC), MIUR under the Contract No. 2010YJ2NYW-010, the ESF Grants No. 8943, No. MJD140, and No. MTT8, by the recurrent financing SF0690030s09 project and by the European Union through the European Regional Development Fund. We would like to thank the Galileo Galilei Institute in Florence for hospitality during the completion of this work.

[1] G. Aad *et al.* (ATLAS Collaboration), Phys. Lett. B **716**, 1 (2012).
[2] S. Chatrchyan *et al.* (CMS Collaboration), Phys. Lett. B **716**, 30 (2012).
[3] F. Hubaut (ATLAS Collaboration), talk at the Moriond 2013 EW session; E. Mountricha (ATLAS Collaboration), talk at the Moriond 2013 QCD session; V. Martin (ATLAS Collaboration), talk at the Moriond 2013 EW session; ATLAS Collaboration, Reports No. ATLAS-CONF-2013-009, ATLAS-CONF-2013-010, ATLAS-CONF-2013-011, ATLAS-CONF-2013-012, ATLAS-CONF-2013-013; ATLAS-CONF-2013-014, and ATLAS-CONF-2013-030.
[4] G. Gomez-Ceballos (CMS Collaboration), talk at the Moriond 2013 EW session; M. Shen (CMS Collaboration), talk at the Moriond 2013 QCD session; B. Mansoulie (CMS Collaboration), talk at the Moriond 2013 EW session; V. Dutta (CMS Collaboration), talk at the Moriond 2013 EW session; CMS Collaboration, Report No. CMS-PAS-HIG-13-001, CMS-PAS-HIG-13-002, CMS-PAS-HIG-13-003, CMS-PAS-HIG-13-004, CMS-PAS-HIG-13-006, and CMS-PAS-HIG-13-009.
[5] L. Živković (CDF and D0 Collaborations), talk at the Moriond 2013 EW session.
[6] P. Fayet, Nucl. Phys. **B90**, 104 (1975).
[7] U. Ellwanger, C. Hugonie, and A. M. Teixeira, Phys. Rep. **496**, 1 (2010).
[8] L. J. Hall, D. Pinner, and J. T. Ruderman, J. High Energy Phys. 04 (2012) 131.

[9] U. Ellwanger, J. High Energy Phys. 03 (2012) 044.
[10] J.-J. Cao, Z.-X. Heng, J. M. Yang, Y.-M. Zhang, and J.-Y. Zhu, J. High Energy Phys. 03 (2012) 086.
[11] K. S. Jeong, Y. Shoji, and M. Yamaguchi, J. High Energy Phys. 09 (2012) 007.
[12] K. Agashe, Y. Cui, and R. Franceschini, J. High Energy Phys. 02 (2013) 031.
[13] G. Belanger, U. Ellwanger, J. F. Gunion, Y. Jiang, S. Kraml, and J. H. Schwarz, J. High Energy Phys. 01 (2013) 069.
[14] K. Choi, S. H. Im, K. S. Jeong, and M. Yamaguchi, J. High Energy Phys. 02 (2013) 090.
[15] S. F. King, M. Muhlleitner, R. Nevzorov, and K. Walz, Nucl. Phys. **B870**, 323 (2013).
[16] R. T. D'Agnolo, E. Kuflik, and M. Zanetti, J. High Energy Phys. 03 (2013) 043.
[17] R. S. Gupta, M. Montull, and F. Riva, J. High Energy Phys. 04 (2013) 132.
[18] T. Gherghetta, B. von Harling, A. D. Medina, and M. A. Schmidt, J. High Energy Phys. 02 (2013) 032.
[19] Z. Kang, J. Li, T. Li, D. Liu, and J. Shu, Phys. Rev. D **88**, 015006 (2013).
[20] C. Cheung, S. D. McDermott, and K. M. Zurek, J. High Energy Phys. 04 (2013) 074.
[21] T. Cheng, J. Li, T. Li, and Q.-S. Yan, arXiv:1304.3182.
[22] M. Badziak, M. Olechowski, and S. Pokorski, J. High Energy Phys. 06 (2013) 043.
[23] B. Bhattacherjee, M. Chakraborti, A. Chakraborty, U. Chattopadhyay, D. Das, and D. K. Ghosh, Phys. Rev. D **88**, 035011 (2013).
[24] U. Ellwanger, J. High Energy Phys. 08 (2013) 077.
[25] R. Barbieri, D. Buttazzo, K. Kannike, F. Sala, and A. Tesi, Phys. Rev. D **87**, 115018 (2013).
[26] P. P. Giardino, K. Kannike, I. Masina, M. Raidal, and A. Strumia, arXiv:1303.3570.
[27] ATLAS Collaboration, ATL-PHYS-PUB-2012-004.
[28] CMS Collaboration, http://indico.cern.ch/contributionDisplay.py?contribId=144&confId=175067. see file CMS-EF-ESPG.pdf.
[29] S. Schael *et al.* (ALEPH Collaboration, DELPHI Collaboration, L3 Collaboration, OPAL Collaboration, LEP Working Group for Higgs Boson Searches), Eur. Phys. J. C **47**, 547 (2006).
[30] M. J. Dolan, C. Englert, and M. Spannowsky, J. High Energy Phys. 10 (2012) 112.
[31] F. Goertz, A. Papaefstathiou, L. L. Yang, and J. Zurita, J. High Energy Phys. 06 (2013) 016.
[32] LEP Higgs Working Group for Higgs boson searches, arXiv:hep-ex/0107034.
[33] CMS Collaboration, Report No. CMS-PAS-HIG-13-016.
[34] R. Barbieri, B. Bellazzini, V. S. Rychkov, and A. Varagnolo, Phys. Rev. D **76**, 115008 (2007).
[35] CMS Collaboration, Report No. CMS-PAS-HIG-12-050.